Dev Genes Evol (2011) 221:17–27
DOI 10.1007/s00427-011-0355-7

ORIGINAL ARTICLE

Decapentaplegic (*dpp*) regulates the growth of a morphological novelty, beetle horns

Bethany R. Wasik · Armin P. Moczek

Received: 28 January 2011 / Accepted: 17 February 2011 / Published online: 12 March 2011

Abstract Studies focusing on the development of morphological novelties suggest that patterning genes underlying traditional appendage development (i.e. mouthparts, legs, and wings) also play important roles in patterning novel morphological structures. In this study, we examine whether the expression and function of a member of the TGF-β signaling pathway, *decapentaplegic* (*dpp*), promotes development of a morphologically novel structure: beetle horns. Beetle horns are complex secondary sexual structures that develop in the head and/or prothorax, lack obvious homology to other insect outgrowths, and vary remarkably between species and sexes. We studied *dpp* expression through in situ hybridization, performed functional analyses with RNA interference, and gathered allometric measurements to determine the role of *dpp* during both pronotal and head horn development in both sexes of two morphologically dissimilar species in the *Onthophagus* genus, *Onthophagus binodis* and *Onthophagus sagittarius*. Our findings show that in addition to affecting growth and patterning of traditional appendages, *dpp* regulates beetle horn growth and remodeling.

Keywords *Decapentaplegic* · Horned beetles · Novelty · *Onthophagus* · RNA interference · Appendage patterning

Communicated by C. Desplan

Electronic supplementary material The online version of this article (doi:10.1007/s00427-011-0355-7) contains supplementary material, which is available to authorized users.

B. R. Wasik (✉) · A. P. Moczek
Department of Biology, Indiana University,
915 E. Third Street, Myers Hall 150,
Bloomington, IN 47405–7107, USA
e-mail: bethany.wasik@gmail.com

Introduction

The development and evolution of morphological novelties continues to represent a major frontier in evolutionary developmental biology. While all traits must descend from some ancestral form, novel traits are often defined as lacking obvious homology to other traits in the same or different organism. How then do novel traits originate? The development of morphological novelties may result from several possible mechanisms, including the evolution of novel genes or gene networks or the recruitment of existing genes and networks into new developmental patterning contexts. Research on the latter possibility has become a starting point to determine how many morphological novelties may have first arisen. For example, genes in appendage patterning networks, studied extensively in the fruit fly, *Drosophila melanogaster*, appear to have been co-opted repeatedly to regulate the development and evolution of several novel morphological structures, such as butterfly eyespots (e.g., Brunetti et al. 2001) or abdominal mating appendages in sepsid flies (Bowsher and Nijhout 2009). In this study, we examine whether the expression and function of a member of the tumor growth factor beta (TGF-β) signaling pathway, *decapentaplegic* (*dpp*), have been co-opted to regulate the development and evolution of morphological structures that are both novel and highly diverse, beetle horns.

Beetle horns are complex secondary sexual structures which develop in two major body regions which normally do not produce outgrowths in insects: the dorsal head and the dorsal prothorax (pronotum). Thousands of beetle species develop horns which vary in size, shape, and location between species, sexes, and alternative morphs within sexes (Arrow 1951). Therefore, beetle horns can be considered evolutionary novelties that have undergone

tremendous diversification since their origin. Although beetle horns lack obvious homology to other insect structures, including traditional appendages, they may be patterned by genes such as *dpp* which normally regulate the growth and development of traditional appendages. For example, beetle horns originate as epidermal outbuddings like legs, wings, and mouthparts and undergo explosive growth during the days immediately preceding the larval to pupal molt (the prepupal growth phase), which is followed by a phase of sculpting, remodeling, and in the case of horns, oftentimes pronounced resorption (the pupal remodeling phase). Final adult expression of horns, like that of traditional appendages, is then the sum of both prepupal growth and pupal remodeling.

Horns and traditional appendages may also share very specific developmental patterning events, like the establishment of the proximodistal (PD) axis. In traditional appendages such as legs or antennae, the establishment of the PD axis is executed cooperatively between *dpp* and *wingless* (*wg*; a ligand in the Wnt signaling pathway) and directed by a segment polarity gene, *hedgehog* (*hh*) (Diaz-Benjumea et al. 1994). *dpp* and *wg* establish mutually repressive expression domains in the dorsal and ventral regions of the developing appendage, respectively, which results in an expression gradient in a distal to proximal direction (Jiang and Struhl 1996; Theisen et al. 1996). Gradient expression of both *dpp* and *wg* promote the formation of mutually antagonistic expression domains of several downstream patterning genes: *Distal-less* (*Dll*) expression in distal appendage regions, *dachshund* (*dac*) expression in medial appendage regions, and *homothorax* (*hth*) expression in proximal-most appendage regions (e.g., Abu-Shaar and Mann 1998; Diaz-Benjumea et al. 1994; Lecuit and Cohen 1997).

The expression and function of *Dll* and *hth* have been studied in the context of *Onthophagus* beetle horn development. Both *Dll* and *hth* are critical for proper PD axis organization in several traditional appendages but also show corresponding expression and function during the development of beetle horns (Moczek and Nagy 2005; Moczek et al. 2006; Moczek and Rose 2009). Given the dependence of *Dll* and *hth* on *wg* and *dpp* signaling, this raises the possibility that interactions between *dpp* and *wg* determine where and how horns develop. Previous insect studies have shown that disrupted or altered *dpp* expression can indeed affect appendage development. For example, misexpression of *dpp* or *wg* in ventral appendages (i.e., legs, antennae, and mouthparts) of *Drosophila* leads to abnormal cell determination in the developing appendage and loss of mutual antagonism, which results in the formation of new PD axes via bifurcation or branching (Campbell et al. 1993; Diaz-Benjumea et al. 1994). In addition to appendage patterning, *dpp* regulates the growth and size of appendages and positioning of joint regions through precise boundaries of expression (reviewed in Affolter and Basler 2007; Manjón et al. 2007; Schwank and Basler 2010). Furthermore, reduced *dpp* signaling during *Drosophila* larval development causes a disruption in cytoskeleton organization that affects cell shape, the degree of cell death, and wing growth (Bryant 1988; Shen and Dahmann 2005).

Here, we investigate *dpp* expression and function in two closely related *Onthophagus* species, *Onthophagus binodis* (Fig. 1a) and *Onthophagus sagittarius* (Fig. 1b), which differ substantially in pronotal and head horn expression. We also explore the role of *dpp* in the development of traditional appendages and sensory structures (i.e., eyes) to better understand the degree of conservation or divergence

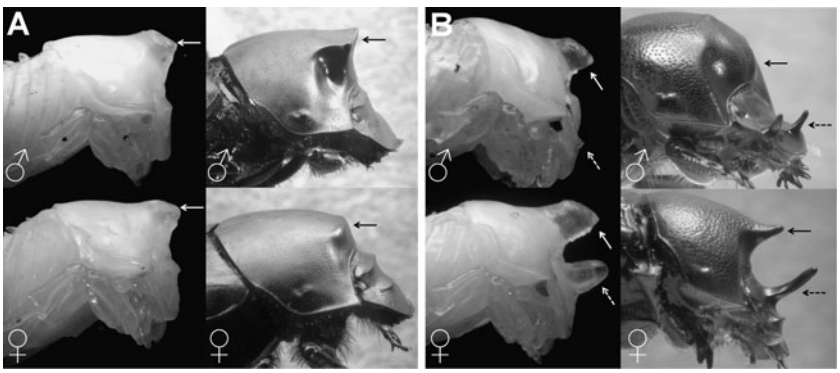

Fig. 1 Pupal and adult horn morphogenesis in *Onthophagus binodis* and *Onthophagus sagittarius*. **a** In *O. binodis*, males and females display monomorphic growth of pronotal horn primordia during the prepupal stage (*white arrows*). Once animals molt into pupae, differential pupal remodeling converts male pronotal horns into future adult outgrowths, whereas female pupal horns are resorbed into a pronotal ridge (*black arrows*). **b** *O. sagittarius*, in contrast, displays two horn types, which differ in their morphogenesis. Pronotal horns develop similar to those in *O. binodis*, showing no major differences in prepupal growth but diverge during the pupal remodeling phase (*white solid arrows*). Here, however, it is the female that retains the pronotal horn into adulthood whereas the male horn is almost completely resorbed (*black solid arrows*). Males and females also express sexually dimorphic head horns (*black dashed arrows*). Sexual dimorphism is already evident in pupae and little remodeling occurs during the pupal stage

of *dpp* function in its ancestral domains of expression. Our results show that *dpp* is expressed and functions in a largely conserved manner during the development of legs, wings, and eyes yet at the same time appears to have acquired an important novel role in the regulation of horn growth during larval and pupal development.

Materials and methods

Rearing conditions

O. binodis was reared as previously described (Moczek et al. 2006; Moczek and Rose 2009), and *O. sagittarius* was reared as described in Wasik et al. (2010). Colony maintenance, breeding and sexing were done as in past studies (Moczek and Nagy 2005).

dpp cloning and sequence analysis

O. binodis dpp (*Obdpp*) was cloned through polymerase chain reaction (PCR) from an *O. binodis* cDNA library using degenerate primers designed to nucleotides encoding amino acids 283–290 and 364–371 in *Tribolium castaneum dpp* (*Tcdpp*; GenBank accession no. NP_001034540). *O. sagittarius dpp* (*Osdpp*) was cloned through nested PCR from cDNA with degenerate forward primers designed to nucleotides encoding amino acids 234–240 and 283–290 and reverse primers designed to nucleotides encoding amino acids 366–371 and 359–365 in *Tcdpp* (Genbank accession no. NM_001039451). The same region was used for dsRNA construction in both species. *Obdpp* and *Osdpp* PCR products were cloned into a pCRII-TOPO vector with TOPO TA Cloning kit (Invitrogen; Carlsbad, CA) and the pSC-A vector with a Strataclone PCR Cloning kit (Stratagene/Agilent; Santa Clara, CA), respectively (also in Moczek and Rose 2009). *Obdpp* and *Osdpp* constructs were sequenced as previously described in Moczek and Rose (2009) and submitted to Genbank (*Obdpp*: HM632025, *Osdpp*: HM632024). Nucleotide and amino acid alignments were generated with Clustal X (Thompson et al. 1997).

In situ hybridization

DIG-labeled (Roche, IN) sense and antisense RNA probes were constructed from the entire isolated sequences for both *Obdpp* (266 bp) and *Osdpp* (252 bp. Probes were synthesized with RNA polymerases using MEGAscript High Yield Transcription Kits (Applied Biosystems/Ambion; TX). RNA probes were used on prepupal sagittal, larval cryo-sections of both *Onthophagus* species, and in situ hybridization was performed as previously described (Moczek et al. 2006).

dsRNA construction and injection

dsRNA constructs for *Obdpp* (266 bp) and *Osdpp* (252 bp) were created from each, entire isolated sequences. In vitro transcription and injection of *Obdpp*, *Osdpp*, and control dsRNA constructs were done as described in Wasik et al. (2010). Animals of both species were injected with dsRNA concentrations between 0.5 and 5 μg/mL initially to determine any relationship between dsRNA concentration and phenotype severity. As no obvious relationship was observed, the remainder and majority of animals were injected with 2.5 μg/mL, as performed in (Wasik et al. 2010). All adults were weighed on the second day of adulthood, preserved in 70% EtOH, and stored at −20°C.

Tissue collection

Thoracic tissue from both species and sexes was collected within 24 h of pupation for wild-type animals and *dpp* RNA interference (RNAi) animals with both morphological and allometric measurement effects (e.g., large abdomens, reduced or no horn tissue, and abnormal leg/mouthpart structures). Tissue was excised with sharp 5 mm scissors (Vannas-Tübingen/FST Inc.; Foster City, CA) in 1X phosphate-buffered saline, placed in RNAse-free tubes (Kontes/VWR; IL), disrupted with RNAse-free pestles (Kontes/VWR; IL) in RLT buffer (Qiagen; RNeasy Mini Kit; Alameda, CA), centrifuged at 4°C, and stored at −80°C until RNA isolation.

RNA extraction and cDNA synthesis

RNA extraction from pupal thoracic tissue was done with reagents from the RNeasy Mini Kit and RNase-Free DNase Set (Qiagen; Alameda, CA) with the following modifications. Upon thawing, tissue samples were centrifuged at 4°C for 10 min at full speed, and the supernatant was combined with an equal volume of 70% EtOH. The mixture was centrifuged in an RNeasy spin column for 2 min at 12,000 relative centrifugal force (rcf). For DNase treatment, buffer RW1 was added to the spin column, centrifuged for 30 s at 12,000 rcf and incubated with diluted DNase I stock with buffer RDD at RT for 15 min. The reaction was terminated with RW1 and centrifuged for 30 s at 12,000 rcf. Buffer RPE was added to the spin column, spun at 12,000 rcf for 30 s, and followed by centrifugation with a new collection tube for 1.5 min at 16,000 rcf. RNA was eluted with 25μL RNase-free water by centrifugation for 1 min at 16,000 rcf. RNA concentrations were collected using a NanoDrop 1000 Spectrophotometer (NanoDrop/Thermo Scientific; Wilmington, DE). cDNA was synthesized using the Quantitect Reverse Transcription Kit (Qiagen; Alameda,

CA), and concentrations were also measured with a NanoDrop 1000 Spectrophotometer (NanoDrop/Thermo Scientific; Wilmington, DE). In *O. binodis*, cDNA from thoracic tissue was collected from five wild-type females and males, and five *dpp* RNAi females and males. In *O. sagittarius*, cDNA from thoracic tissue was collected from four wild-type females and males, and four *dpp* RNAi females and males.

Quantitative RT-PCR analyses

Primers used for quantitative reverse transcriptase PCR (RT-PCR) were designed using Oligoanalyzer and PrimerQuest/Primer3 (Integrated DNA Technologies; Rozen and Skaletsky 1998) and are listed in Table 1 in the Electronic supplementary materials. Primers were tested with pooled cDNA samples from both species to measure effective reaction concentration, and standard curve measurements were done with each quantitative RT-PCR run. Negative controls in both primer tests and quantitative RT-PCR reactions included no template (water) and non-reverse-transcribed RNA. cDNA samples were prepared in 250 ng/μL concentrations and used with the SYBR Green PCR Kit (Qiagen; Alameda, CA). Quantitative RT-PCR reactions were performed with a Stratagene MX3000P system (Stratagene/Agilent; Santa Clara, CA) using SYBR Green and ROX dyes for fluorescence readings and ROX as the reference dye. The thermal profile used was as follows. Segment 1 was 1 cycle at 95°C for 15 min. Segment 2 was 50 cycles that encompassed a 15-s decline to 94°C, 30 s at 58°C, and 30 s at 72°C with endpoint data collection. Segment 3 was one cycle starting with 1 min at 95°C, followed by 30 s at 55°C, and ending with 30 s at 95°C with an all points data collection between 55°C and 95°C. Quantitative RT-PCR of all tissue was replicated, and results were analyzed using MxPro software (Stratagene/Agilent; Santa Clara, CA). Threshold values were automatically determined by the MxPro software (v. 4.0, Build 367, Schema 80; Stratagene/Agilent; Santa Clara, CA) but were corrected to the mean threshold value of replicate reactions for accurate expression level comparisons (see Cappelli et al. 2008). Two-tailed *t* tests were used to determine whether *dpp* expression levels (normalized to actin, $C_{t\ dpp}/C_{t\ actin}$) were significantly different among wild-type and *dpp* RNAi individuals for each species (as described in Barmina and Kopp 2007). Relative expression fold differences were determined using the $2^{-\Delta\Delta C_t}$ equation (Livak and Schmittgen 2001; Schmittgen and Livak 2008). Specifically, C_t values of tissue from both wild-type and *dpp* RNAi were inputted so $\Delta\Delta C_t = \left(C_{t\ dpp} - C_{t\ actin}\right)_{wild-type} - \left(C_{t\ dpp} - C_{t\ actin}\right)_{dpp\ RNAi}$. C_t values were averaged for each treatment group (n=5 for *O. binodis* and n=4 for *O. sagittarius*).

Allometric measurements

Pupae and adults from all treatments were measured as described in Moczek and Rose (2009). However, prothorax width was used an indicator of both pupal and adult size, due to artifactual larger body mass following *dpp* RNAi in pupae and adults. Pronotal and head horns (*O. sagittarius*) were measured using the same microscope set-up as previously described (Moczek et al. 2006). Eye width was measured using the average width of the left and right dorsal eye regions on the dorsal head surface. All measurements were recorded to the nearest 0.001 mm and graphed using SigmaPlot software (v. 7.0, SPSS Inc., Chicago, IL).

Pupal measurements were used among all treatments to evaluate the effect, if any, of *dpp* RNAi on prepupal horn growth. However, as outlined in the introduction, adult horn development is also affected by pupal resorption, which may be affected independently by *dpp* RNAi. Thus, to determine any changes in adult horn length from pupal resorption, two additional analyses were conducted using individual pupal and adult measurements. First, the degree of "absolute horn loss" was calculated by subtracting the final adult horn length from the pupal horn length in an individual to compare the degree of resorption among individuals in each treatment group. Second, "relative horn loss" was calculated as the relative difference (%) between pupal and adult horn length. Combined, these measurements helped distinguish between RNAi-induced effects on prepupal horn growth and pupal horn resorption and their respective contributions to final adult horn length.

Statistical analyses

All ANOVAs were conducted with JMP (v. 4.0, SAS Institute Inc., NC). Pronotal and head horn length, as well as relative and absolute horn loss, were used as response variables while prothorax width, treatment (RNAi or control-injected), and *width x treatment* interactions were used as model effects. Only measurements from adults with obvious *dpp* RNAi phenotypes were used for RNAi treatment analyses. The same approach was used to examine possible treatment effects on adult prothoracic fore-tibia length and adult eye width. Wild-type and control-injected animals did not differ significantly in any measurements, unless otherwise noted in the results.

Results

Onthophagus *dpp* cloning and sequence analysis

We cloned a 266 bp *dpp* fragment from *O. binodis* and a 252 bp *dpp* fragment from *O. sagittarius* that correspond to

amino acids 284–371 and 284–366 in *Tc*dpp, respectively (Genbank accession no. NP_001034540). Both *Onthophagus dpp* sequences were within the protein-coding Hin region of *dpp* and contained several conserved elements (St Johnston et al. 1990). Firstly, five of seven conserved cysteine residues that are important for homodimer formation were conserved in the protein encoded by *Obdpp*, and four of seven were conserved in the *Osdpp* protein sequence (Fig. 1B in the Electronic supplementary materials; reviewed in Kingsley 1994). Secondly, a conserved 48 bp *dpp* TGF-β signature that encodes amino acids 290–305 in *Tc*dpp was present in both *Onthophagus* sequences (Fig. 1B in the Electronic supplementary materials; Hulo et al. 2006). *Ob*dpp and *Os*dpp proteins shared 95.2% amino acid similarity to each other and 69.3% and 68.6% each to *Tc*dpp, respectively. Additionally, the *Os*dpp protein had a unique, single lysine (K) insertion between amino acids 356 and 357 of *Tc*dpp.

Onthophagus *dpp* mRNA expression

In both species and sexes, *dpp* mRNA was expressed in regions of the larval epidermis undergoing growth of both head and thoracic structures (Figs. 2AB (*O.b.*) and 2CD (*O.s.*) in the Electronic supplementary materials). Specifically, *dpp* mRNA was expressed throughout developing mouthparts, pronotal horn, wing, gut, and leg tissue in both species and sexes. Furthermore, *dpp* mRNA was expressed in head horn tissue in *O. sagittarius* (data not shown). Negative controls with similar tissue sections and body regions displayed no *dpp* mRNA expression (Fig. 2b (inset)).

Quantitative RT-PCR analyses

Our quantitative RT-PCR results indicated a relative decrease of *dpp* in tissue from *dpp* RNAi individuals compared with *β-actin* in the same tissue sample, relative to *dpp* and *β-actin* levels in wild-type tissue samples. Specifically, *dpp* transcript levels in *O. binodis* male and female thoracic tissue following RNAi were 1.40- and 1.75-fold lower (respectively) than *dpp* levels in wild-type, relative to *β-actin* transcript levels. In *O. sagittarius*, *dpp* transcript levels in males and females following RNAi were 1.12- and 1.19-fold lower (respectively) than *dpp* levels in wild-type, relative to *β-actin* transcript levels. These results indicated we were successful in reducing the amount of *dpp* transcription in thorax tissue by larval RNAi in *O. binodis* with a more subtle decrease in *O. sagittarius*. Then, using two-tailed *t* tests, we found normalized *dpp* expression levels ($C_{t\ dpp}/C_{t\ actin}$) were significantly different ($p<0.05$) between *O. binodis* wild-type and *dpp* RNAi tissue samples. However, there was no significant difference (data not shown) between *O. sagittarius* wild-type and *dpp* RNAi tissue samples, despite very obvious and consistent RNAi phenotypes at least in part similar to those seen in *O. binodis* (described below). This result suggested that while we failed to detect a significant reduction of *Osdpp* transcripts in our statistical analyses, reduction of *Osdpp* transcripts was sufficient to generate obvious and interpretable phenotypes.

dpp RNAi

In both species, we observed that the location of ds*dpp* injection did not influence the resulting RNAi phenotypes.

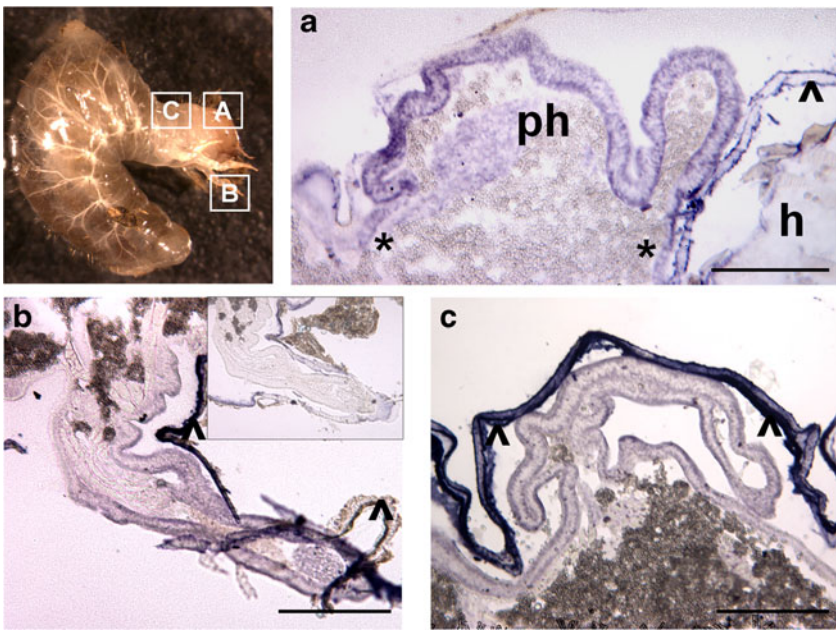

Fig. 2 *Onthophagus dpp* mRNA Expression. *dpp* in situ hybridization on sagittal cryo-sections from prepupal *Onthophagus binodis* and *Onthophagus sagittarius* larvae (*top left* is reference) using *Obdpp* and *Osdpp* RNA probes, respectively (visualized as *purple* stain in tissue). In all images, dorsal is *up*, anterior is *right*, and posterior is *left*. *dpp* expression is observed throughout **a** the pronotal horn (*ph*); *h* head; *asterisks* denote boundaries of *dpp* expression in the pronotal horn, **b** legs; *top right inset* shows no signal in control leg section, **c** wing primordium. *Carets* denote artefactual labeling in overlaying cuticle. *Scale bars* represent 200 μm

Survival and penetrance of control-injected and RNAi animals are detailed in Table 2 in the Electronic supplementary materials. Both species displayed many similar RNAi phenotypes, including phenotypes similar to those seen in *dpp* characterization studies of *Drosophila* mutants, such as a cleft in the medial anterior prothorax (notal cleft), missing distal appendage regions, ectopic or bifurcating antennae, shortened elytra, abnormal fore-tibia and claw development, and reduced or absent mouthparts (Fig. 3; Segal and Gelbart 1985; Spencer et al. 1982). We used the presence of any or all the above-mentioned phenotypic effects to determine which individual adults were likely affected by *dpp* RNAi. For the remainder of our results and discussion, we focus our data analysis on affected adults, pupae that developed into affected adults and pupae that died prior to phenotype characterization. Measurements from pupae that developed into adults lacking any of the phenotypes described above were not incorporated into our analyses. Below, we first describe our results for traditional appendages and eyes, structures whose development is known to be regulated in part by *dpp*. Then, we describe our results for both pronotal and head horns as putative novel targets of *dpp* signaling.

O. binodis

We injected 351 *O. binodis* larvae with ds*dpp* and obtained 138 adults. Of the resulting adults, 106 had morphological effects (76.8%) consistent with a reduction in *dpp* function (Table 2 in the Electronic supplementary materials). The only phenotypic effects we observed in pupae were pupal appendages either held tightly against the body wall or partially covered by wings. Predominant adult phenotypes included abnormal or fused antennal segments, notal clefts, reduced elytra, slightly abnormal distal leg development, reduced or missing structures in the labium (labial palps and hypopharyngeal sclerites), reduced or missing palps along with bifurcated galea in the maxilla, larger elongated abdomens compared with wild-type or control-injected adults (Fig. 3a–i). Furthermore, male and female fore-tibia length were significantly reduced following *dpp* RNAi ($p<0.0001$; Fig. 3 and Table 3 in the Electronic supplementary materials). We also detected a small, yet significant effect of control injections alone on fore-tibia length in females but not males, when compared with the wild-type animals ($p=0.0008$). However, *dpp* RNAi fore-tibia length remained significantly shorter regardless of comparison to wild-type or control-injected individuals ($p<0.0001$). Additionally, we observed a significant reduction in dorsal eye width in both male and female *dpp* RNAi adults ($p<0.0001$; Fig. 4 and Table 4 in the Electronic supplementary materials).

O. sagittarius

We injected 261 *O. sagittarius* larvae with ds*dpp* which resulted in a total of 86 adults; 22 adults displayed morphological effects (25.6%) indicative of reduced *dpp* function (Table 2 in the Electronic supplementary materials). In *O. sagittarius* pupae affected by *dpp* RNAi, we observed all legs were shortened and abnormally folded against the ventral body wall, and mouthpart structures protruded noticeably further outward from the head capsule than in wild-type or control pupae. In adults, predominant *dpp* RNAi phenotypes included fused or bifurcated antennal segments, dorsal cleft formation, reduced elytra, abnormal leg development including proximal bifurcation of the coxa, reduced or missing labial structures, and reduced palps and bifurcated galea in the maxilla (a subset of these phenotypes are shown in Fig. 3l–q). Fore-tibia length of *O. sagittarius* was significantly reduced in both males and females following *dpp* RNAi, compared with fore-tibia length in control-injected animals ($p<0.001$; Fig. 3 and Table 3 in the Electronic supplementary materials). Furthermore, dorsal eye width did not show a significant reduction in *O. sagittarius* adults (Fig. 4 and Table 4 in the Electronic supplementary materials).

dpp RNAi effects on prepupal pronotal horn growth

We quantified *dpp* RNAi effects on prepupal pronotal horn growth by comparing pupal pronotal horn lengths from *dpp* RNAi animals and control-injected animals using analysis of variance of morphometric measurements (Fig. 4a–b). In *O. binodis*, the length of pupal pronotal horns was significantly reduced in both males and females after *dpp* RNAi compared with that in control-injected individuals ($p<0.0001$; Fig. 4c; Table 5 in the Electronic supplementary materials). We also detected a small but significant effect in pronotal horn length in control-injected females, but not males, when compared with the wild-type individuals ($p=0.0313$; Fig. 4c; Table 5 in the Electronic supplementary materials). However, pronotal horn length measurements from *dpp* RNAi individuals were significantly reduced regardless of whether they were compared with wild-type or control-injected individuals ($p<0.0001$). In *O. sagittarius*, pupal horn length was also significantly affected in both *dpp* RNAi females and males when compared with pupal horn length in control-injected animals ($p<0.0001$; Fig. 4a–c; Table 5 in the in the Electronic supplementary materials). Therefore, our data suggest *dpp* regulates prepupal pronotal horn growth in both *O. binodis* and *O. sagittarius* species, regardless of sex.

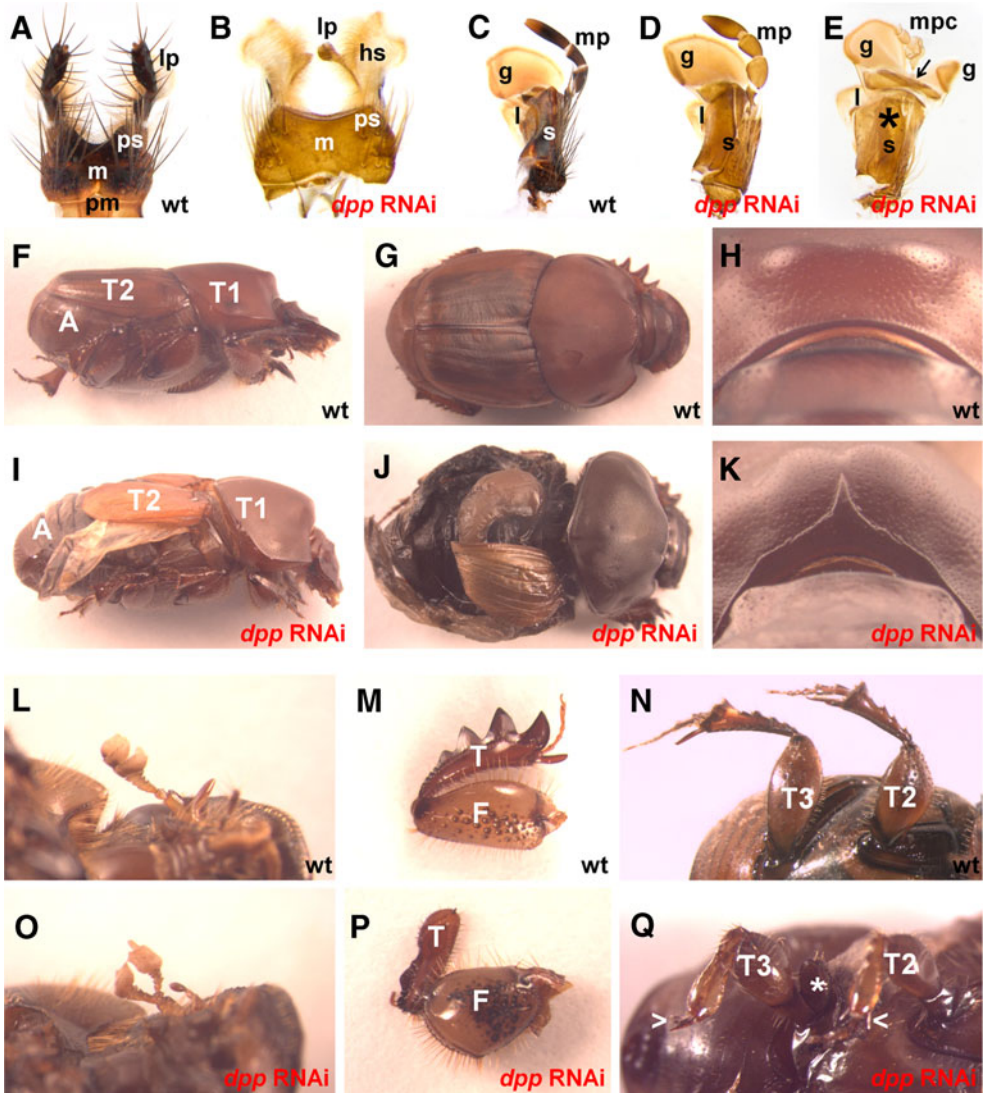

Fig. 3 *Onthophagus binodis* and *Onthophagus sagittarius* non-horn *dpp* RNAi phenotypes. Shown are representative non-horn *dpp* RNAi phenotypes in *O. binodis* (**a**–**k**) and *O. sagittarius* (**l**–**q**). **a** Wild-type labial mouthpart structures composed of labial palps (*lp*) and hypopharyngeal sclerites (hidden behind labial palps). Both structures are attached to the postmentum (*ps*) which connects to the mentum (*m*), and prementum (*pm*). **b** *dpp* RNAi labial mouthpart structures with reduced and abnormal lp, broad hypopharyngeal sclerites (*hs*), and a reduced ps. **c**)Wild-type maxillary mouthpart structures composed of galea (*g*), lacinia (*l*), and maxillary palp (*mp*) connected by a base structure (*s* stipes). **d** A mild *dpp* RNAi maxillary mouthpart phenotype with stout mp and a broader s. **e**)A severe *dpp* RNAi maxillary mouthpart phenotype with a bifurcation of the g denoted by *black arrow*, with the maxillary palp cuticle (maxillary palp was removed for clarity) in the middle (*mpc*). *Asterisk* denotes very broad s. **f** Wild-type female from lateral view (*T1* prothorax, *T2* elytra/forewings/mesothorax, *A* abdomen). **g** Wild-type female from dorsal view. **h** Wild-type pronotum. **i** *dpp* RNAi female with reduced T2 and larger A. **j** *dpp* RNAi female with abnormal elytra from dorsal view. **k** *dpp* RNAi pronotum with notal cleft. **l** *O. sagittarius* wild-type antennae. **m** Wild-type prothoracic leg (*T* tibia, *F* femur). **n** Wild-type mesothoracic (T2) and metathoracic (*T3*) legs. **o** *dpp* RNAi antennal bifurcation. **p** *dpp* RNAi prothoracic leg with reduced and abnormal T. **q** *dpp* RNAi T2 and T3 legs with ectopic proximal leg bud denoted with an *asterisk* and rotated carets denoting reduced distal leg regions. Anterior is right and posterior is left in all images, where applicable. Photo credit for **a**–**e** is Dr. Franck Simonnet

dpp RNAi effects on pupal pronotal horn remodeling

Next, we examined whether *dpp* RNAi-induced changes in pupal horn length were followed by altered patterns of pupal horn resorption. In *O. binodis*, we detected a significant decrease in absolute and relative pupal horn loss in both sexes of *dpp* RNAi individuals, compared with control individuals ($p<0.0001$; Table 6 in the in the

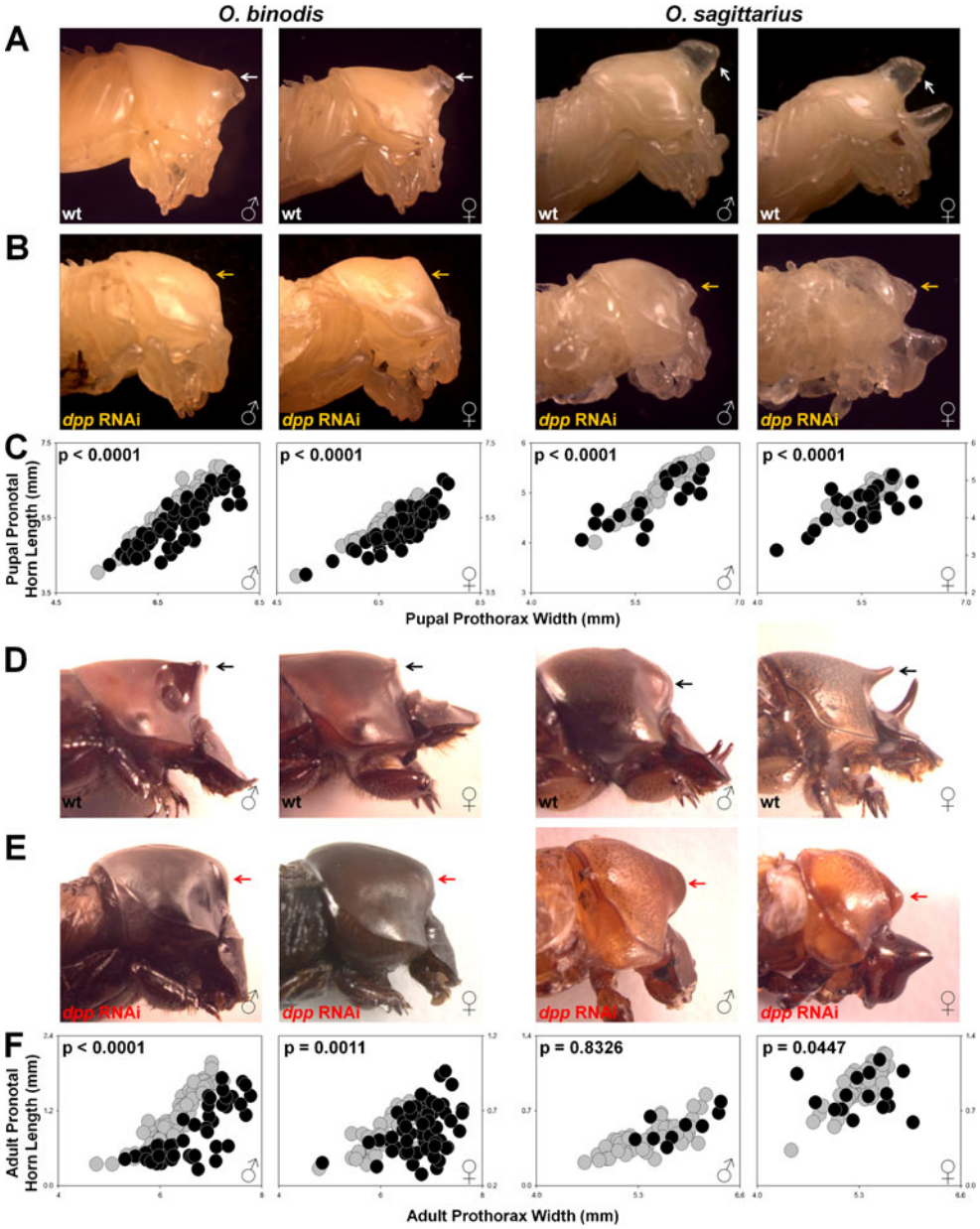

Fig. 4 *Onthophagus binodis* and *Onthophagus sagittarius* pronotal horn phenotypes and allometries. In all rows, *left to right* columns display *O. binodis* males, *O. binodis* females, *O. sagittarius* males, and *O. sagittarius* females. In all images, anterior is *right* and posterior is *left*, and pronotal horns are denoted by *solid arrows*. **a** Wild-type pupal pronotal horn phenotypes. **b** Representative *dpp* RNAi pupal pronotal horn phenotypes. **c** Scaling relationship between pupal prothorax (*x*-axis) and pupal pronotal horn length (*y*-axis) for control-injected individuals (*gray circles*) and ds*dpp*-injected individuals (*black circles*). **d** Wild-type adult pronotal horn phenotypes. **e** Representative *dpp* RNAi adult pronotal horn phenotypes. **f** Scaling relationship between adult prothorax (*x*-axis) and pronotal horn length (*y*-axis) (see Table 5 in the Electronic supplementary materials)

Electronic supplementary materials). We also observed a similar effect in female, but not male *O. sagittarius* individuals (absolute: $p=0.0130$, relative: $p=0.0181$; Table 6 in the Electronic supplementary materials). Thus, in these three cases (*O. binodis* males, females, and *O. sagittarius* females), the effect of *dpp* RNAi on pupal horn resorption counteracted the reduction in pronotal horn growth during the prepupal stage.

dpp RNAi effects on adult pronotal horn development

Adult pronotal horn length in *O. binodis* was significantly reduced in both males ($p<0.0001$) and females ($p=0.0011$; Fig. 4d–f; Table 5 in the Electronic supplementary materials) following *dpp* RNAi. This observation, along with our pupal horn resorption analyses above, suggests reduced prepupal horn growth was not fully compensated by reduced horn loss during the pupal remodeling stage in *dpp* RNAi individuals. In contrast, *O. sagittarius* adult pronotal horn length was only minimally reduced in females ($p=0.0447$) but not in males (p=ns; Fig. 4d–f; Table 5 in the Electronic supplementary materials). This suggests that the RNAi-induced reduction in horn growth detected during the prepupal stage of *O. sagittarius* was largely compensated by reduced horn loss during the pupal remodeling stage.

dpp RNAi effects on head horn development

Finally, we measured the effect of *dpp* RNAi on head horn length in *O. sagittarius* to determine whether horns in

different locations were affected similarly by reduced *dpp* expression. We found no significant effect on pupal head horn length in *O. sagittarius* males ($p=0.7012$) and a trend towards reduced head horn length in the resulting male adults ($p=0.0582$). However, a visual inspection of the data set suggested that unlike male pupae, nearly half of the affected male adults actually exhibited a substantial reduction in head horn length. In females, we found a consistent, border-line significant effect of *dpp* RNAi on head horn length in both pupae ($p=0.0467$) and adults ($p=0.0420$; Fig. 5 and Table 7 in the Electronic supplementary materials). Analyses of both absolute and relative head horn loss were not significant in either sex of *O. sagittarius*, indicating no change in the degree of head horn resorption after *dpp* RNAi (data not shown).

Discussion

In this study, we show that a member of the TGF-β signaling pathway, *dpp*, regulates the development of an evolutionary novelty, beetle horns. Specifically, we find that *dpp* RNAi reduces prepupal pronotal horn growth but increases the retention of pupal horn tissue into the adult stage by reducing pupal horn resorption. Furthermore, we find evidence that *dpp* RNAi affects prepupal growth, but not pupal resorption of head horns. Lastly, and in agreement with past functional *Onthophagus* studies (Moczek and Rose 2009; Simonnet and Moczek 2011; Wasik et al. 2010), we illustrate that appendage patterning networks are active beyond embryogenesis and affect the expression of both novel and traditional adult morphological features. Together, these results suggest that differential co-option of *dpp* function may contribute to the development of beetle horns, without compromising the ancestral function of *dpp* in the regulation of growth and patterning of traditional appendages and eyes. Below we briefly discuss the implications of our most significant results.

dpp regulates growth and remodeling of pronotal horns and growth but not remodeling of head horns

Our results show that *dpp* is expressed during the development of pronotal and head horns and that *dpp* RNAi significantly reduces prepupal horn growth uniformly in two species (Fig. 5). Together, these observations suggest that *dpp* regulates the growth of pronotal and head horns during the prepupal stage. We also observed that during the pupal stage, *dpp* RNAi counteracted the reduction in pronotal, but not head, horn growth from the prepupal stage (Fig. 5). Specifically, *O. binodis* males, females, and *O. sagittarius* females exhibited a significant reduction in both absolute and relative pupal pronotal horn loss in both sexes of *dpp* RNAi individuals. Combined, these observations suggest decreased *dpp* transcript levels during the larval and early pupal stages affect horn remodeling in pronotal horns only. The effect of *dpp* on pupal horn remodeling may reflect direct *dpp*-mediated regulation of horn remodeling, possibly through the regulation of programmed cell death (PCD). In fact, PCD has recently been documented as a possibly important contributor to pupal remodeling of pronotal horns (Kijimoto et al. 2010; Moczek 2006). Alternatively, a reduction in pupal horn resorption may reflect the compensatory action of other developmental pathways without direct regulatory input of *dpp*. Further studies are needed to distinguish between these two possibilities.

dpp regulates growth of traditional non-horn appendages

We observed non-horn phenotypes in response to *dpp* RNAi in *O. binodis* and *O. sagittarius* which collectively paralleled *Drosophila dpp* mutant phenotypes (e.g., Spencer et al. 1982). Our results match those of previous studies, revealing RNAi phenotypes that tend to fall into two classes: appendage size reduction and/or the establishment of an additional PD axis.

Size reduction has been associated with *dpp* misexpression in various insect appendages, and primary phenotypes include changes in appendage shape and size and also increased localized PCD (reviewed in Schwank and Basler 2010). While we did not measure the amount of PCD in this study, it is a plausible mechanism for the decrease in fore-tibia, elytra, and eyes in *Onthophagus* beetles in response to *dpp* RNAi. The second potential mechanism is the establishment of a second PD axis in the absence of *dpp* signaling which results in the bifurcation of antennae, legs, and maxillary galea structures. When *dpp* expression is reduced during development, the mutually antagonistic relationship between *dpp* and *wg* is disrupted, and *wg* expression is no longer restricted to its established domain (Jiang and Struhl 1996; Theisen et al. 1996). As a result, the expression of downstream patterning genes, such as *Dll* and *aristaless* (*al*), expand to other regions of the appendage and promote the formation of an additional PD axis (Campbell et al. 1993; Diaz-Benjumea et al. 1994). Our results agree with this hypothesis as well as past interpretations of *dpp* mutant phenotypes (e.g., Spencer et al. 1982). However, a more thorough investigation of *wg* expression or downstream patterning gene expression (i.e., *Dll*, *dac*, *hth*, and *al*) will be necessary to further evaluate our observations.

Overall, our results suggest that a combination of both appendage size reduction and PD axis alteration mechanisms are consequences of larval *dpp* RNAi in *Onthophagus* beetles, and we conclude that traditional appendages in

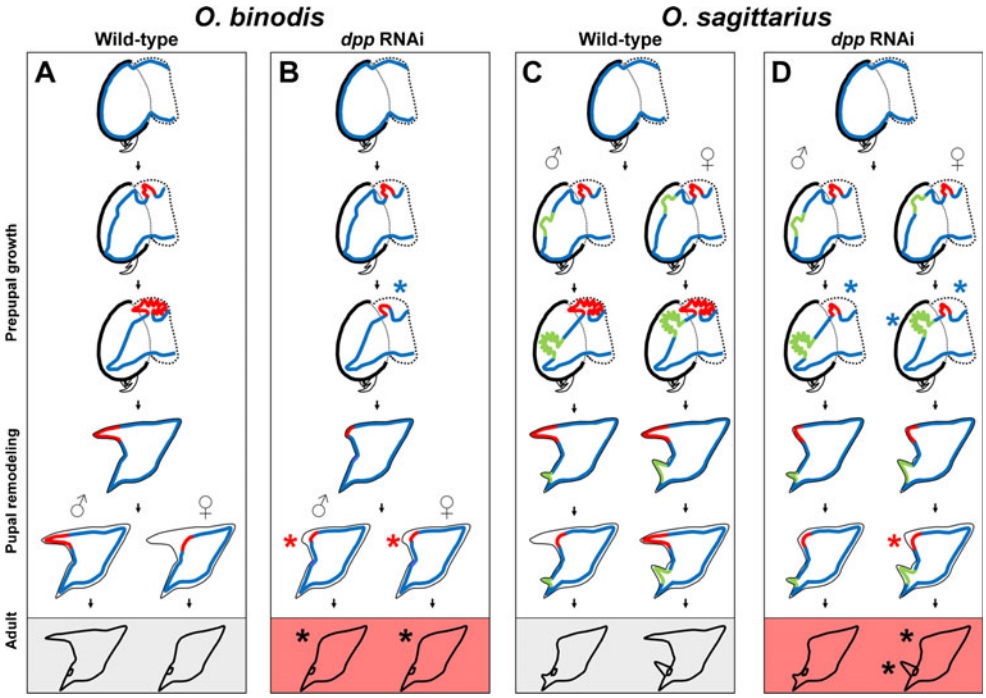

Fig. 5 Summary of *dpp* RNAi effects on pronotal and head horn development in *O. binodis* and *O. sagittarius*. In all columns, *top to bottom* illustrates pronotal and head horn development from larva to adult. *Black* indicates larval and pupal cuticle, *blue* represents epidermal tissue, and *red* and *green* represent pronotal and head horn tissue, respectively. *Colored asterisks* indicate statistically significant changes in pupal horn length (*blue*), pupal horn remodeling (*red*), or adult horn length (*black*). **a** Pronotal horn development in wild-type *O. binodis*. Males and females show similar prepupal growth of horn tissue but differ in the degree of horn resorption, such that horns are only retained in males. **b** *dpp* RNAi reduces pronotal horn growth as well as pupal horn resorption in both sexes, resulting in adults with significantly shorter horns in both sexes. **c** Pronotal and head horn development in wild-type *O. sagittarius*. Males and females show similar prepupal growth of horn tissue but differ in the degree of horn resorption, such that horns are only retained in females. **d** *dpp* RNAi results in reduced *O. sagittarius* prepupal horn growth in both sexes and decreased pupal horn resorption in females. In head horns, only females show decreased prepupal growth and decreased adult head horn length

Onthophagus beetles are affected by *dpp* RNAi similar to what has been reported in prior studies. Interestingly, we observed consistent, species-specific distributions of phenotypes and severity in our results. For example, fore-tibia and elytra length were significantly reduced in both species, but eye width was affected only in *O. binodis*. Also, we observed the establishment of an additional PD axis in maxillary mouthparts in both species, but legs and antenna were only affected in *O. sagittarius*. These differences may result from artefactual differences in RNAi efficiency or instead may reflect subtle, evolved differences in *dpp* function between the two species, as discussed below.

Firstly, differences in RNAi phenotypes between *O. binodis* and *O. sagittarius* may simply result from differences in developmental time or body size. Both species in this study were injected with nearly identical ds*dpp* constructs (Fig. 1B in the Electronic supplementary materials), but the larval and pupal stages of *O. binodis* are nearly twice as long as those of *O. sagittarius*, resulting in significant body size differences between both species. Specifically, adult *O. sagittarius* are substantially smaller in body size than *O. binodis*, and changes in *dpp* expression may be more acute in smaller individuals, perhaps explaining the greater severity of *O. sagittarius* phenotypes. Alternatively, diverged interactions between *dpp* and downstream target genes may affect the response in appendage and horn patterning to *dpp* RNAi, creating a species-specific effect in the observed phenotypes. For example, recent studies in *Drosophila* have shown plasticity in the TGF-β signaling pathway and that a gene duplication event produced a novel ligand, *Screw* (*Scw*) that has both novel and conserved interactions with other pathway members (Fritsch et al. 2010). These observations suggest that components of the TGF-β signaling pathway are capable of diversifying quickly, and further characterization of other TGF-β signaling pathway genes in both *Onthophagus* species, in addition to upstream regulators such as *hedgehog* (*hh*), may elucidate a mechanism for the species-specific effects seen here.

Acknowledgments We would like to thank David Angelini for providing primer sequences, Franck Simonnet for mouthpart dissection and imaging, Justin Kumar for access to a NanoDrop 1000 Spectrophotometer, and the Center for Genomics and Bioinformatics at Indiana University for quantitative RT-PCR resources. We would

also like to thank Erin Yoder for expert beetle care and Will Haines for collecting and sending *O. sagittarius* from the field. Finally, we thank Emilie Snell-Rood and Amy Cash for constructive feedback and helpful comments on earlier versions of these results. This research was carried out while BRW was supported through NIH Genetics Training Grant (2T32 GMOO7757-29) and NSF-IGERT Grant (DGE-0504627). Additional support was provided by NSF grants IOS 0445661 and IOS 0718522 to APM.

References

Abu-Shaar M, Mann R (1998) Generation of multiple antagonistic domains along the proximodistal axis during *Drosophila* leg development. Development 125:3821–3830

Affolter M, Basler K (2007) The Decapentaplegic morphogen gradient: from pattern formation to growth regulation. Nat Rev Genet 8:663–674

Arrow GJ (1951) Horned beetles, a study of the fantastic in nature. W. Junk, The Hague

Barmina O, Kopp A (2007) Sex-specific expression of a *HOX* gene associated with rapid morphological evolution. Dev Biol 311:277–286

Bowsher J, Nijhout H (2009) Partial co-option of the appendage patterning pathway in the development of abdominal appendages in the sepsid fly *Themira biloba*. Dev Genes Evol 219:577–587

Brunetti CR, Selegue JE, Monteiro A, French V, Brakefield PM, Carroll SB (2001) The generation and diversification of butterfly eyespot color patterns. Curr Biol 11:1578–1585

Bryant P (1988) Localized cell death caused by mutations in a *Drosophila* gene coding for a transforming growth factor-beta homolog. Dev Biol 128:386–395

Campbell G, Weaver T, Tomlinson A (1993) Axis specification in the developing *Drosophila* appendage: the role of wingless, decapentaplegic, and the homeobox gene aristaless. Cell 74:1113–1123

Cappelli K, Felicetti M, Capomaccio S, Spinsanti G, Silvestrelli M, Supplizi A (2008) Exercise induced stress in horses: selection of the most stable reference genes for quantitative RT-PCR normalization. BMC Mol Biol 9:49

Diaz-Benjumea F, Cohen B, Cohen S (1994) Cell interaction between compartments establishes the proximal-distal axis of *Drosophila* legs. Nature 372:175–179

Fritsch C, Lanfear R, Ray RP (2010) Rapid evolution of a novel signalling mechanism by concerted duplication and divergence of a BMP ligand and its extracellular modulators. Dev Genes Evol 220(9–10):235–250

Hulo N, Bairoch A, Bulliard V, Cerutti L, De Castro E, Langendijk-Genevaux P, Pagni M, Sigrist C (2006) The PROSITE database. Nucleic Acids Res 34:D227–D230

Jiang J, Struhl G (1996) Complementary and mutually exclusive activities of decapentaplegic and wingless organize axial patterning during Drosophila leg development. Cell 86:401–409

Kijimoto T, Andrews JR, Moczek AP (2010) Programmed cell death shapes the expression of horns within and between species of horned beetles. Evol Dev 12(5):449–458

Kingsley D (1994) The TGF-beta superfamily: new members, new receptors, and new genetic tests of function in different organisms. Genes Dev 8:133–146

Lecuit T, Cohen S (1997) Proximal–distal axis formation in the *Drosophila* leg. Nature 388:139–145

Livak K, Schmittgen T (2001) Analysis of relative gene expression data using real-time quantitative PCR and the 2(−Delta Delta C (T)) method. Methods 25:402–408

Manjón C, Sánchez-Herrero E, Suzanne M (2007) Sharp boundaries of Dpp signalling trigger local cell death required for *Drosophila* leg morphogenesis. Nat Cell Biol 9:57–63

Moczek AP (2006) Pupal remodeling and the development and evolution of sexual dimorphism in horned beetles. Am Nat 168:711–729

Moczek AP, Nagy LM (2005) Diverse developmental mechanisms contribute to different levels of diversity in horned beetles. Evol Dev 7:175–185

Moczek AP, Rose DJ (2009) Differential recruitment of limb patterning genes during development and diversification of beetle horns. Proc Natl Acad Sci USA 106:8992–8997

Moczek AP, Rose D, Sewell W, Kesselring BR (2006) Conservation, innovation, and the evolution of horned beetle diversity. Dev Genes Evol 216:655–665

Rozen S, Skaletsky HJ (1998) Primer3. Available at: http://www-genome.wi.mit.edu/genome_software/other/primer3.html

Schmittgen T, Livak K (2008) Analyzing real-time PCR data by the comparative C(T) method. Nat Protoc 3:1101–1108

Schwank G, Basler K (2010) Regulation of organ growth by morphogen gradients. Cold Spring Harb Perspect Biol 2:a001669

Segal D, Gelbart W (1985) Shortvein, a new component of the decapentaplegic gene complex in *Drosophila melanogaster*. Genetics 109:119–143

Shen J, Dahmann C (2005) Extrusion of cells with inappropriate Dpp signaling from *Drosophila* wing disc epithelia. Science 307:1789–1790

Simonnet F, Moczek AP (2011) Conservation and diversification of gene function during mouthpart development in *Onthophagus* beetles. Evol Dev (in press)

Spencer F, Hoffmann F, Gelbart W (1982) Decapentaplegic: a gene complex affecting morphogenesis in *Drosophila melanogaster*. Cell 28:451–461

St Johnston R, Hoffmann F, Blackman R, Segal D, Grimaila R, Padgett R, Irick H, Gelbart W (1990) Molecular organization of the decapentaplegic gene in *Drosophila melanogaster*. Genes Dev 4:1114–1127

Theisen H, Haerry T, O'Connor M, Marsh J (1996) Developmental territories created by mutual antagonism between Wingless and Decapentaplegic. Development 122:3939–3948

Thompson JD, Gibson TJ, Plewniak F, Jeanmougin F, Higgins DG (1997) The CLUSTAL_X windows interface: flexible strategies for multiple sequence alignment aided by quality analysis tools. Nucleic Acids Res 25:4876–4882

Wasik BR, Rose DJ, Moczek AP (2010) Beetle horns are regulated by the *Hox* gene, Sex combs reduced, in a species- and sex-specific manner. Evol Dev 12:353–362